Angewandte Chemie
Eine Zeitschrift der Gesellschaft Deutscher Chemiker

Supporting Information

Transcription Factor Based Small-Molecule Sensing with a Rapid Cell Phone Enabled Fluorescent Bead Assay

*Margaret Chern, Padric M. Garden, R C. Baer, James E. Galagan, and Allison M. Dennis**

ange_202007575_sm_miscellaneous_information.pdf

Materials and Methods

Materials: Red emitting Qdot™ 655 ITK Organic Quantum Dots were sourced from ThermoFisher Scientific (Q21721MP). Synthesis of green QDs required cadmium oxide (CdO), zinc acetate ($Zn(Ac)_2$), selenium pellets (Se), sulfur (S), oleic acid (OA), oleylamine (Olam), and trioctylphophine (TOP). Reagents used for CL4 synthesis included lipoic acid (LA), ethylenediamine (EDA), 1,1'-carbonyldiimidazole (97%) (CDI) , methyl acrylate, lithium hydroxide (LiOH), and sodium borohydride ($NaBH_4$). The solvents used in our experiments were chloroform ($CHCL_3$), methanol (MeOH), ethanol (EtOH), hexanes (Hex) and octadecene (ODE). Chemicals and solvents purchased from Sigma Aldrich and used without further purification. Bovine Serum Albumin (Fisher BP9706-100), Streptavidin-Agarose from *Streptomyces avidinii* (Sigma-Aldrich: S1638), DNA custom ordered from IDT (www.idtdna.com), and 1× PBS (Gibco) were used in bioassays. QDs in water were stored in 1× Borate Buffer diluted from a 20× stock purchased from Thermo Fisher. Analytes: Anhydrotetracycline hydrochloride (Cayman 10009542), doxycycline hyclate (Sigma Aldrich D9891). Serum for complex media testing: Fetal Bovine Serum (Corning 35015CV).

QD Synthesis: Green-emitting QDs were synthesized using a slightly modified one-pot method previously described by the Lee lab.[1,2] Cadmium oleate and zinc oleate were made with a 1:4 cation to oleic acid ratio by reacting either CdO or $Zn(Ac)_2$ with OA at 150 °C and diluting to a final cation concentration of 0.2 M with ODE. The anion precursor was made by dissolving Se and S into the same TOP solution at final concentrations of 0.13 M and 1.3 M, respectively, by gently heating at 90 °C. Once made, 5 mL of 0.2 M $Zn(OA)_2$ and 0.4 mL of $Cd(OA)_2$ were loaded into a 100 mL round bottom flask (rbf) and heated to 300 °C. Once the cation solution reached 300 °C, 2 mL of the TOP:Se:S solution was quickly injected and reacted for 15 mins before being taken off the heating mantle and allowed to cool naturally to room temperature. The resulting QDs were ~10 nm in diameter with an emission maximum at 505 nm. All synthesis steps up to this point were performed using standard air-free conditions. Once synthesized, QDs were stored in their native solution.

CL4 synthesis: Compact ligand 4 (CL4), first described by the Medintz lab,[3] was synthesized exactly as described in a previous report.[4] Briefly, the carboxylic acid on LA was coupled with EDA in a CDI mediated reaction. The resulting compound was purified using column chromatography. Methyl acrylate was added to the terminal primary amine via Michael additionand the resulting product purified and concentrated before re-dispersing in a 2:1 ethanol/water mixture. Ester hydrolysis and di-thiol cleavage were then performed successively by adding LiOH and $NaHB_4$, respectively. Excess ethanol was evaporated off and the resulting CL4 in H_2O solution stored under argon at 4 °C as a ~760 mM solution, ready for use.

QD ligand exchange: Water-solubility was conferred to both the red and green QDs by exchanging their native ligands with CL4. First, the QDs were precipitated from their storage solutions by diluting with Hex and adding EtOH and MeOH. The resulting solution is turbid and the QDs pelleted through centrifugation (3 mins at 21,000 rcf). The clear supernatant containing unreacted precursors and excess ligands was discarded and the pellet redispersed in $CHCl_3$. CL4 was then added in sufficient amounts to provide 3,000 CL4 molecules per nm^2 of QD surface. QD phase transfer is immediate, but the solution was mixed for at least 1 hr under argon to ensure stability of the thiol binding to the QD surface. Once ligand exchanged, the QD/water phase was decanted and filtered through a 0.1 µm PVDF syringe filter. The QDs were then buffer exchanged 3× into 1× Borate buffer using 30 kDa Amicon spin filters and stored as concentrated as possible at 4 °C.

Biotin labeling of green QDs: Green-emitting QDs (505 nm) were synthesized and ligand exchanged with CL4 as described above. The terminal carboxyl groups on the CL4 were reacted with biotinylated-amine from a commercially available kit (G-Biosciences BS16). In a typical reaction, 0.1 nmol of QD/CL4 was mixed with 20 µL of 1-Ethyl-3-(3-dimethylaminopropyl)carbodiimide (EDC, 1 mg/mL) and 30 µL of N-Hydroxysuccinimide (NHS, 1mg/mL) in 2-(N-morpholino)ethanesulfonic acid (MES) buffer, pH 7.0. The solution is mixed and sonicated for 2 hours. QD precipitates were removed with centrifugation and the pH of the remaining solution adjusted to 7.5 before addition of 5 µL of amine-biotin dissolved at 1 mg/mL in MES, pH 7.5. This was left to stir overnight at 4 °C before concentrating and buffer exchanging the QD stock using a 30 kDa Amicon spin filter.

TetR(D) plasmid construction: The TetR(D) C-His coding sequence was ordered codon optimized from IDT with necessary 5' and 3' fusion sequences for cloning into the pETite C-His Kan expression plasmid (Lucigen). DNA was cloned into the linearized plasmid per the manufacturer's protocol with no adjustments.

Synthesized TetR(D) gene sequence

GAAGGAGATATACATATGGCACGTTTGAACCGCGAGTCAGTCATCGATGCGGCCCTGGAG
CTGCTTAACGAGACGGGGATCGACGGTCTGACCACACGCAAGCTTGCTCAAAAATTAGGT
ATTGAACAGCCGACGCTGTACTGGCACGTAAAAAACAAGCGTGCTTTGCTTGATGCCTTGG
CCGTCGAAATTTTAGCCCGCCACCACGATTATTCCCTGCCCGCAGCTGGAGAATCATGGC
AGTCGTTTTTACGCAACAATGCCATGTCGTTCCGTCGCGCACTTTTGCGTTACCGTGACGG
GGCTAAGGTCCACCTGGGGACCCGCCCCGACGAGAAGCAGTATGATACGGTGGAAACGC
AGCTTCGTTTCATGACAGAGAATGGGTTTAGCCTTCGTGATGGCTTATATGCTATCTCCGC
GGTATCGCATTTTACGCTTGGGGCGGTACTGGAGCAACAGGAACATACGGCCGCCTTGAC
GGATCGCCCGGCTGCTCCCGATGAAAACTTGCCACCGTTACTGCGTGAGGCCCTGCAAAT
TATGGATAGCGACGATGGTGAACAGGCGTTTCTGCATGGTTTGGAGTCTCTTATTCGTGGT
TTCGAGGTGCAGTTGACTGCGCTGCTTCAGATCGTTGGAGGAGATAAACTGATTATCCCAT
TCTGCGGATCTCATCATCACCACCATCAC

TetR Expression and Purification: The plasmid for the TetR(D) protein was transformed into competent BL21(DE3) *E.coli* (New England Biolabs) for IPTG-induced protein expression. The his-tagged TetR was purified using a nickel-nitrilotriacetic acid (Ni-NTA) agarose column as previously described.[6,7] In the same publication, we report the TetR-*tetO* binding affinities for the same protein and DNA sequence as used here, determined using biolayer interferometry: K_D = 7.32 ± 0.78 × 10^{-10} M; K_{on} = 184 ± 6.5 × 10^3 $M^{-1}s^{-1}$; K_{off} = 13.4 ± 1.4 × 10^{-5} s^{-1}.[6,7]

DNA Hybridization: The DNA sequences listed in Table S1 were purchased from Integrated DNA Technologies (IDT, https://www.idtdna.com/pages). Biotinylated cognate sequences (bt-*tetO*) and biotinylated scrambled sequences (bt-Sbd) were mixed at a 1:1 molar ratio with their complements in 1× duplex buffer (IDT: 11-05-01-03) and heated to 95 °C for 2 minutes and slowly cooled to room temperature. The hybridized stocks were aliquoted and stored at -20 °C. Once thawed for use, DNA stocks were stored at 4 °C to avoid repeated freeze-thaw cycles. Unfrozen aliquots stored at 4 °C for up to 3 weeks were used without noticeable difference in functionality.

Table S1. DNA Sequences

Label	Sequence[a]	Ref[b]
bt-*tetO*	/5Biosg/GTCA**TCCCTATCA**TT**GATAGAGA**TACTG	[8]
c*tetO*	CAGTAT**CTCTATCA**A**TGATAGGGA**TGAC	[8]
bt-Sbd	/5Biosg/GAAACCGAGCGAGGGACACG	
cSbd	CGTGTCCCTCGCTCGGTTTC	

[a] *tetO* binding motif shown in bold; [b] Reference for the *tetO* binding sequence (bold), spacers and scrambled sequences were randomly chosen in our group.

Bead Assays: In all experiments described in the main paper, QD concentration is kept constant while TF concentration is modulated from 1, 2, 4 and 8× that of the QD. SBs come in a 50% bead/liquid slurry. This ratio is preserved when labeling with bt-DNA (0.2 nmol DNA per every 50 µL beads/liquid slurry) and mixed at a 1:1 volume ratio with TF/QD solutions such that the final bead/liquid composition was 25%. TF/QD stocks were made such that the QD concentration was 100 nM and the final concentration 50 nM after mixing with the SBs. All QD/SB mixtures were washed by replacing the supernatant with clean 1X PBS + 1% (w/v) BSA three times. After the final wash step, half of the amount of liquid was added such that the washed slurry had the same 50% bead density as the commercial stock. The washed bead slurry was distributed to 200 µL PCR tubes in 50 µL aliquots.

Anhydrotetracycline was stored concentrated (2.85 mg/mL) in EtOH at -20 °C and diluted into 1× PBS for use; titrations were prepared at 2× the desired assay analyte concentration. 50 µL of diluted aTc was added to each PCR tube, bringing the assay to 100 µL with 25% SBs and 25 nM QD.

For the two-color assays, a large stock of green beads was prepared by incubating biotin-labeled green QDs (100 µL @ 500 nM) with 1 mL of SB slurry. Any excess unbound QDs were washed from the supernatant. Red sensors using a 2× TF/QD ratio were prepared as described above with increasing amounts of green beads added to adjust the final sensor R/G ratio to ~ 4:1, 2:1, and 1:1. The number of red beads for each R/G ratio was constant.

Image Acquisition and Analysis: Bead assays were imaged by illuminating the PCR tubes with a UV-Lamp (367 nm) under a cardboard box and taking images with a cell phone camera (Samsung Galaxy S6 edge+). JPEG images were loaded into MatLab (MatLab R2019b, MathWorks) and examined in separate red, green, and blue color channels. Irregular pentagons and quadrilaterals were drawn around the bead and supernatant regions of interest (ROIs) and their coordinates saved. Histograms of the image intensities were examined in each of the color channels. Scattering from stray lint particles was observed to exhibit abnormal high intensity in the blue channel; these outlier pixels were eliminated from the ROIs in all three of the color channels. For each ROI, the average and standard deviation of the middle 50% of the pixel intensities calculated for each color channel. Where color channel ratios are reported, the ratios were calculated on a pixel-by-pixel basis before averaging. Where the ratio of the red channel liquid-to-bead regions are reported, the averages were divided and error propagation used to calculate the standard deviation. Averages and standard deviations were used to calculate the 95% confidence intervals displayed in Figure 3.

Using Igor Pro (v. 6.37, WaveMetrics, Inc.), plotted intensity value data were fit to the Hill equation:[9]

$$f(x) = base + \frac{(max - base)}{\left[1 + \left(\frac{EC_{50}}{x}\right)^{rate}\right]}$$

where $f(x)$ is the sensor response at analyte concentration x, EC_{50} is the analyte concentration halfway between the highest signal (max) and lowest signal ($base$), and $rate$ is the slope at the steepest part of the curve.

Detection of Doxycycline and Validation in Complex Media: A concentrated doxycycline stock (10 mM) was made by dissolving doxycycline hyclate in deionized water; these were aliquoted into individual use stocks and stored at -20 °C. Fetal bovine serum (FBS, Corning) was aliquoted into individual use stocks and stored at -20 °C.

Assays were performed as previously described in the one-color format. 50 µL of the resulting supernatants were transferred to a black-walled, clear-bottom, 384-well plate (Corning) for photoluminescence measurements on a SpectraMax M5 plate reader using 260 nm excitation with a 610 nm cutoff filter for emission. Calibration curves derived from known analyte dilutions in buffer were fitted to the Hill function.

For dilution linearity experiments, samples were prepared by diluting FBS five-fold in buffer with either 100 nM anhydrotetracycline, 100 nM doxycycline, or water (no analyte control) spiked in. These samples were then serially diluted to make 10, 50 and 100X dilute samples. Sample concentrations were interpolated from the calibration curve fit function, with samples reading below the limit of detection (three standard deviations above the zero-analyte calibrator) assigned to the limit of detection concentration.

The dilution linearity was assessed to examine the matrix effects of serum on the sensor. To calculate the spike and recovery, a measure of assay accuracy in complex media, the difference between the interpolated concentration of the spiked and unspiked samples was divided by the expected concentration and converted to a percentage.

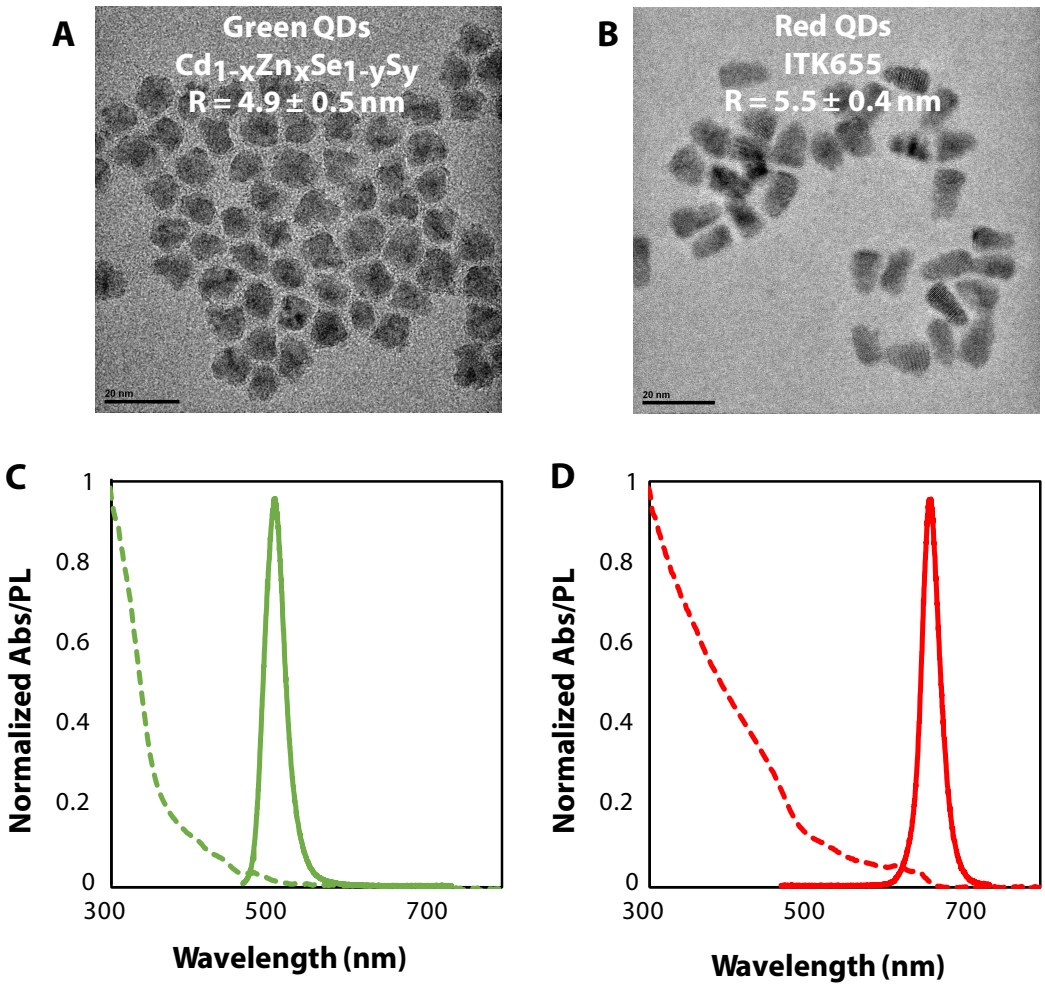

Figure S1. QD Characterization. TEM images of **(A)** green-emitting $Cd_{1-x}Se_{1-y}Zn_xS_y$ one-pot gradient alloy QDs synthesized in-house and **(B)** red-emitting ITK655 (Thermo Fisher). Scale bar = 20 nm. Plots of normalized absorbance and photoluminescence spectra of **(C)** green QDs and **(D)** red QDs.

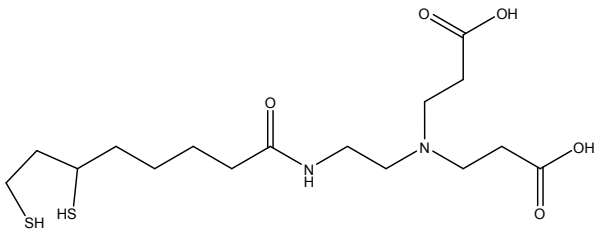

Figure S2. Chemical structure of 3,3'-((2-(6,8-dimercaptooctanamindo)ethyl)azanediyl)-diproprionic acid, also known as compact ligand 4 (CL4). The dithiol binds to the metal-ion surface of the QDs, displacing its native ligands. CL4 is a zwitterion comprised of a primary amine and two carboxyl groups. The ligand confers water solubility and stability to QDs at pHs ranging from 5-13.

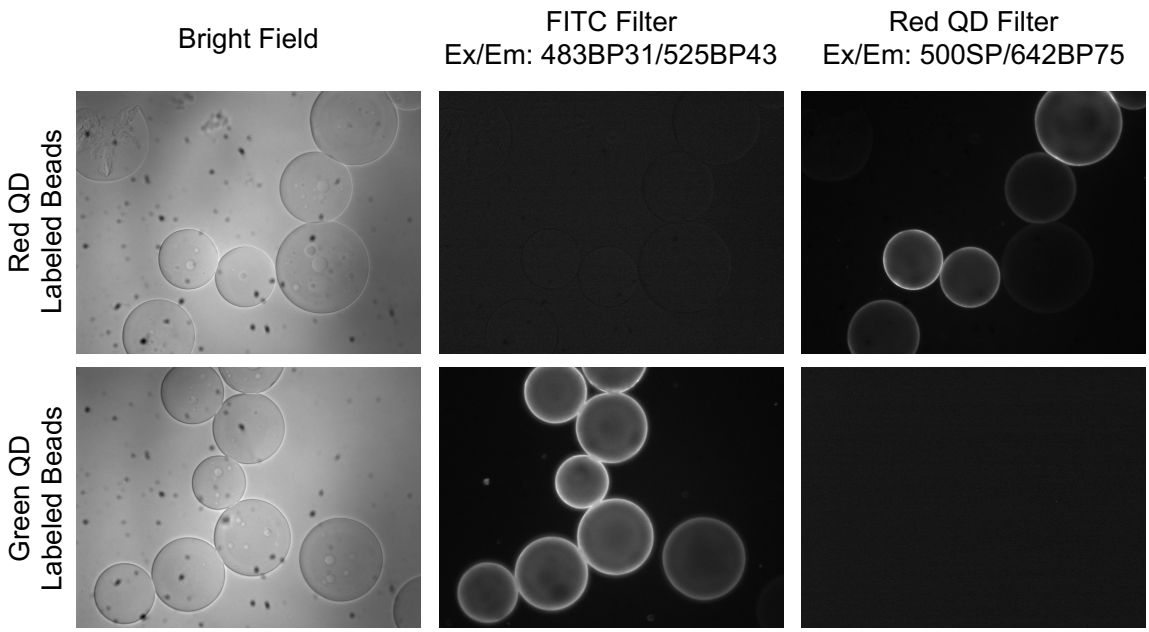

Figure S3. Fluorescent microscope images streptavidin-coated beads (SB) labeled with green and red QDs taken at 40× magnification. Beads labeled with red QDs are observed with a filter set using a 500 nm short pass excitation filter and a 642 nm bandpass emission filter. Conversely, beads labeled with green QDs are visible using a FITC filter cube with a 483 bandpass excitation filter and a 525 bandpass emission filter. The "ring-like" fluorescence localization on the beads indicates that the QDs are localized on the surface of the beads.

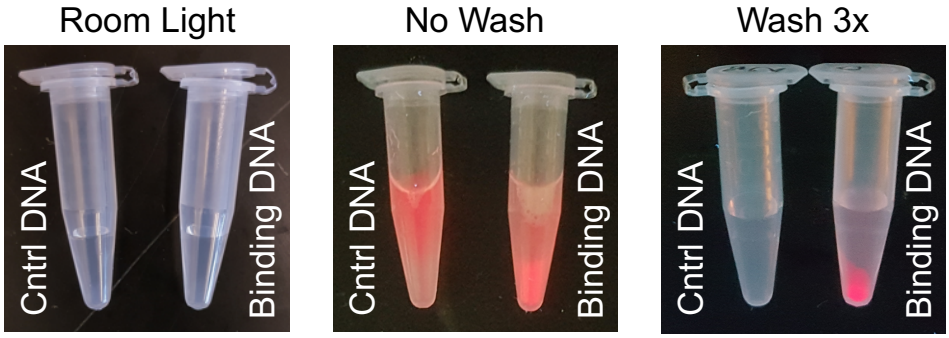

Figure S2. QD-SB Washing. Excess QDs removed by exchanging the supernatant 3× with 1× PBS + 1% (w/v) BSA. The QDs are too dilute to be discerned under the room light. Under UV illumination, one can see QDs colocalizing with the beads when binding DNA is used with excess found in the supernatant, while the beads with control, non-binding DNA show less colocalization with the QDs. After washing the beads to remove unbound QDs, the beads with the control DNA exhibit no fluorescence, while the beads with binding DNA fluoresce red from the bound QDs.

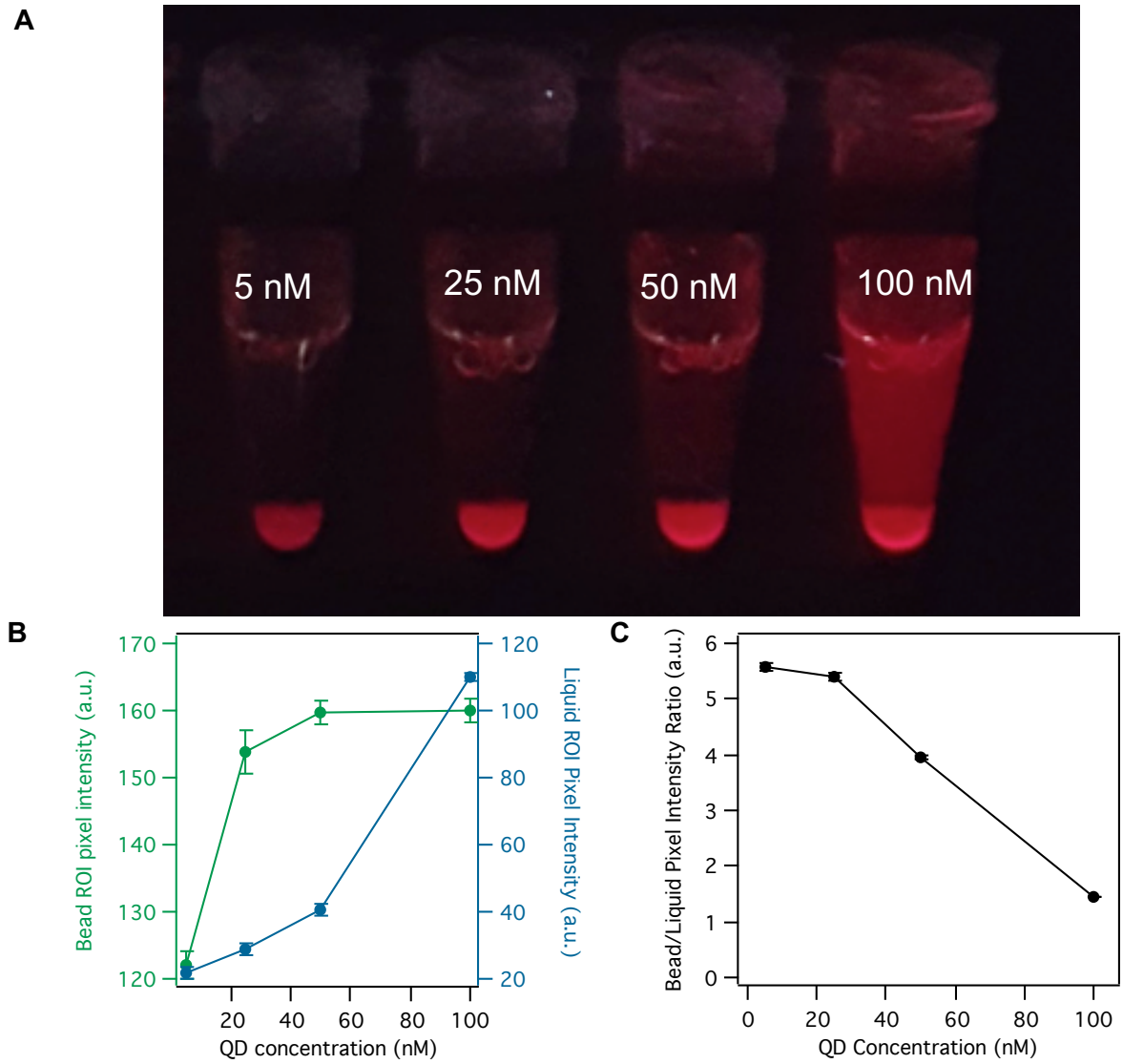

Figure S3. Saturating QD Loading. (**A**) Image showing impact of QD concentration on bead binding using QDs with 8× TFs per QD. With the SB-DNA concentrations held constant, the DNA/TF ratio decreases from 20 to 2.5 as the final QD concentration is increased from 5 nM to 100 nM. (**B**) Average red channel intensity for the bead and liquid fractions of the tubes imaged in (A). (**C**) Ratio of the bead to liquid red-channel intensity in the tubes imaged in (A).

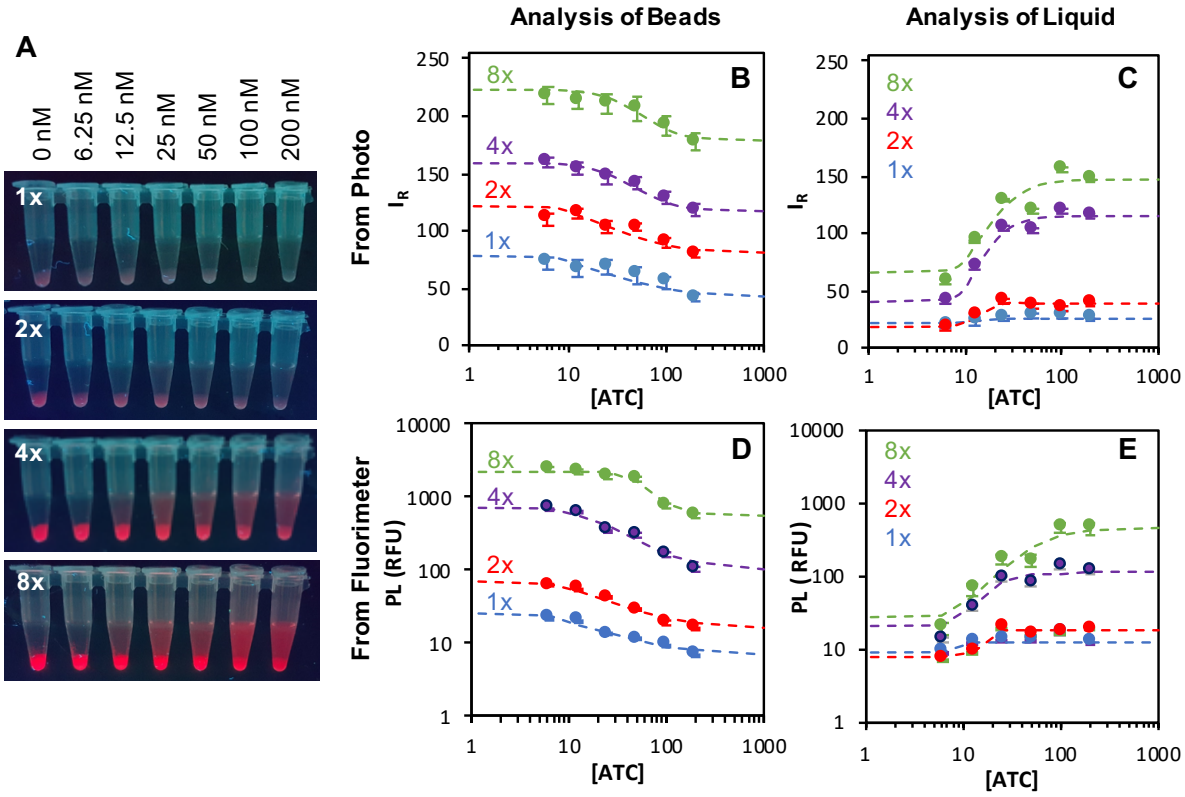

Figure S6: Digital image and spectrophotometer measurements are well correlated. (**A**) Digital images of samples used for the comparative analytics. The tube rows labeled 1, 2, 4, and 8× indicate the TetR/QD ratio used for a given titration series with 0-200 nM aTc added to each column of tubes, as noted above the image. The red channel intensity from the (**B**) bead pellet or (**C**) supernatant region of the image is plotted against aTc concentration. The spectrophotometer-based photoluminescence (PL) measurement of the (**D**) bead pellet or (**E**) supernatant plotted against aTc concentration. Note that the PL intensities are plotted on a log scale for easy comparison to the image-based analyses, as the image intensities in the 8-bit image are already on a log scale with an output between 0 and 255.

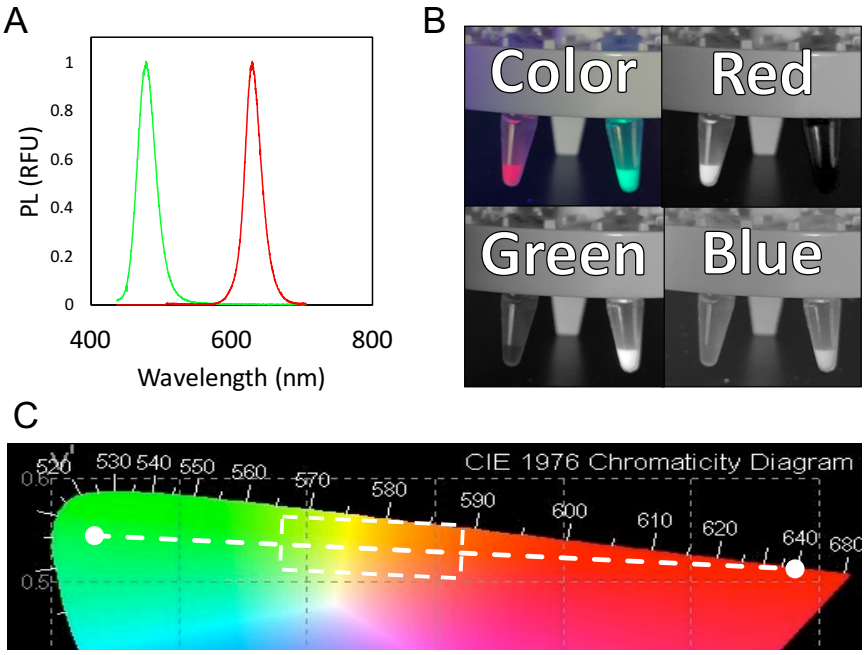

Figure S7. Choice of Colors for Ratio-metric Sensor. Normalized PL spectra of the green emitting and red emitting QDs (**A**) show no emission overlap. An image of two QDs bound to SBs and stored in separate tubes was taken and its color channels split using ImageJ (**B**). While there is effectively no red emission in the green channel, the green QDs show fluorescence in the blue channel. (**C**) The QD emission colors mapped to the CIE 1976 chromaticity diagram. The line connecting the green and red dots indicates the possible colors that can be made by combining the red and green QDs at different ratios. Green was specifically chosen as it can produce the "rainbow" colors when mixed with red.

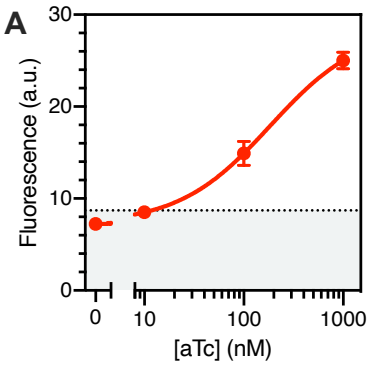

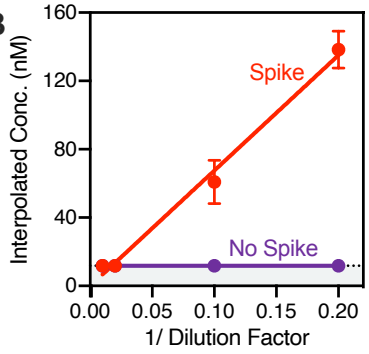

C

Spike and Recovery			
Dilution Factor	Recovered Conc. (nM)	Expected Conc. (nM)	Recovery
5X	126.5 ± 10.9	100	126 ± 11%
10X	49.1 ± 12.7	50	98 ± 25%
50X	Undet.	-	-
100X	Undet.	-	-

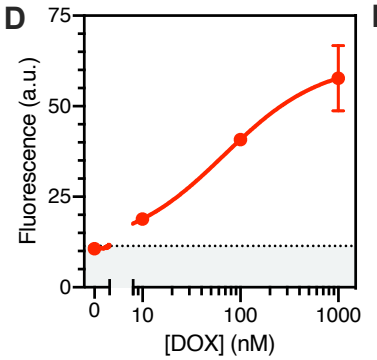

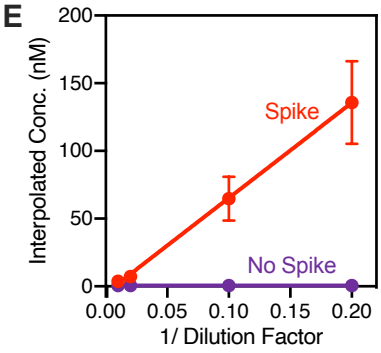

F

Spike and Recovery			
Dilution Factor	Recovered Conc. (nM)	Expected Conc. (nM)	Recovery
5X	135.3 ± 30.7	100	135 ± 31%
10X	64.3 ± 16.1	50	129 ± 32%
50X	6.8 ± 3.1	10	68 ± 31%
100X	3.3 ± 0.2	5	67 ± 3%

Figure S8. Sensor Use in Serum and Detection of Doxycycline. (**A**) Calibration curve of sensor for anhydrotetracycline in plate reader format. Fluorescence is that of the supernatant after assay completion. Shaded region indicates the limit of detection. (**B**) Dilution linearity experiment detecting aTc in fetal bovine serum. Demonstrates that interpolated concentration linearly correlates with dilution factor, indicating minimal matrix effects. (**C**) Spike and recovery results for the dilution linearity experiment. (**D**) Calibration curve for doxycycline. (**E**) Dilution linearity for doxycycline. (**F**) Spike and recovery for doxycycline. aTc experiments performed in triplicate, DOX experiments performed in duplicate. Values below the LOD were assigned to the LOD when interpolating concentrations.

References:

(1) Bae, W. K.; Char, K.; Hur, H.; Lee, S. Single-Step Synthesis of Quantum Dots with Chemical Composition Gradients. *Chem. Mater.* **2008**, *20* (2), 531–539. https://doi.org/10.1021/cm070754d.

(2) Ki Bae, W.; Kwak, J.; Park, J. W.; Char, K.; Lee, C.; Lee, S. Highly Efficient Green-Light-Emitting Diodes Based on CdSe@ZnS Quantum Dots with a Chemical-Composition Gradient. *Adv. Mater.* **2009**, *21* (17), 1690–1694. https://doi.org/10.1002/adma.200801908.

(3) Susumu, K.; Oh, E.; Delehanty, J. B.; Blanco-Canosa, J. B.; Johnson, B. J.; Jain, V.; Hervey, W. J.; Algar, W. R.; Boeneman, K.; Dawson, P. E.; Medintz, I. L. Multifunctional Compact Zwitterionic Ligands for Preparing Robust Biocompatible Semiconductor Quantum Dots and Gold Nanoparticles. *J. Am. Chem. Soc.* **2011**, *133* (24), 9480–9496. https://doi.org/Doi 10.1021/Ja201919s.

(4) Chern, M.; Nguyen, T. T.; Mahler, A. H.; Dennis, A. M. Shell Thickness Effects on Quantum Dot Brightness and Energy Transfer. *Nanoscale* **2017**, *9* (42), 16446–16458. https://doi.org/10.1039/C7NR04296E.

(5) Iverson, S. V; Haddock, T. L.; Beal, J.; Densmore, D. M. CIDAR MoClo: Improved MoClo

Assembly Standard and New E-Coli Part Library Enable Rapid Combinatorial Design for Synthetic and Traditional Biology. *Acs Synth. Biol.* **2016**, *5* (1), 99–103. https://doi.org/10.1021/acssynbio.5b00124.

(6) Nguyen, T. T.; Chern, M.; Baer, R. C.; Galagan, J.; Dennis, A. M. A Förster Resonance Energy Transfer-Based Ratiometric Sensor with the Allosteric Transcription Factor TetR. *Small* **2020**, 1907522. https://doi.org/10.1002/smll.201907522.

(7) Nguyen, T.; Chern, M.; Baer, R. C.; Fan, A.; Grazon, C.; Galagan, J.; Dennis, A. M. QD-FRET-Based Biosensing of Small Molecule Analytes Using Transcription Factor-DNA Binding; Parak, W. J., Osiński, M., Eds.; SPIE, 2019; Vol. 10892, p 25. https://doi.org/10.1117/12.2516576.

(8) Saenger, W.; Hinrichs, W.; Orth, P.; Schnappinger, D.; Hillen, W. Structural Basis of Gene Regulation by the Tetracycline Inducible Tet Repressor–Operator System. *Nat. Struct. Biol.* **2000**, *7* (3), 215–219. https://doi.org/10.1038/73324.

(9) Gadagkar, S. R.; Call, G. B. Computational Tools for Fitting the Hill Equation to Dose-Response Curves. *J. Pharmacol. Toxicol. Methods* **2015**, *71*, 68–76. https://doi.org/10.1016/j.vascn.2014.08.006.